Technobius Physics, 2025, 3(1), 0026, DOI: https://doi.org/10.54355/tbusphys/3.1.2025.0026

Technobius Physics

https://technobiusphysics.kz/

e-ISSN 3007-0147

Article

Synthesis and research of optical and electrical properties of tin dioxide nanoprolocs in the SiO_2/Si track template

Diana Junisbekova*, Zein Baimukhanov, Alma Dauletbekova

Faculty of Physics and Technical Sciences, L.N. Gumilyov Eurasian National University, Astana, Kazakhstan
*Correspondence: diana911115@gmail.com

Abstract. This work presents a study of the structural, optical and electrical characteristics of tin dioxide (SnO_2) nanowires obtained by chemical deposition (CD) into SiO2/Si track templating (templating synthesis). Latent tracks in the SiO2 layer were created by irradiation with fast heavy ions (FHE) Xe at 200 MeV energy with fluence F = 108 cm-2 followed by etching in 4% aqueous hydrofluoric acid (HF) solution. The selected XO method is widely used for the deposition of semiconductor oxide nanowires in SiO_2 nanopores. The CW method is cost-effective because it does not require any special equipment for the deposition of nanowires. To realize the deposition, a solution of metal coordination compound and reducing agent is used. To analyze the pore filling after CW process, the surface morphology of the samples was investigated using Zeiss Crossbeam 540 scanning microscope. The crystallographic structure of SnO2/SiO2/Si nanostructures with SnO_2 nanopore filling was investigated by X-ray diffraction. X-ray diffraction analysis (XRD) is performed on a Rigaku SmartLab X-ray diffractometer. A SnO_2-NP/SiO_2/Si nanostructure with orthorhombic crystalline structure of SnO_2 nanowires supplemented with metallic tin was obtained. The photoluminescence spectra were measured under excitation with 5.17 eV wavelength light using a CM2203 spectrofluorimeter. Gaussian decomposition of the photoluminescence spectra of SnO2-NP/SiO_2/Si structures, showed that they have low intensity, which is mainly due to the presence of defects such as oxygen vacancies, interdomain tin or tin with damaged bonds. The electrical characterization study was carried out using a VersaStat 3 patentiostat. The WAC measurement of the nanowire obtained by chemical deposition showed that due to the presence of metallic tin, the conductivity is close to metallic.
Keywords: SiO_2/Si track templating; chemical deposition; SnO_2 nanowires, tin dioxide; templating synthesis.

1. Introduction

With the manifestation of special properties of various nanoscale objects, a great interest in their research has arisen in recent years. Depending on the application, materials with different functional properties are selected. Today's technologies make it possible to control the morphology of such materials at the nanoscale in order to obtain a large variety of nanostructures (NS) with desired properties [1], [2], [3].

One of the simplest ways to form nanomaterials is the use of nanoporous templates (matrices) [4], [5], [6]. Using this method, different structures can be obtained due to the self-organization of materials of this class inside the pores. The use of pores allows to obtain nanoparticles, nanorods, nanofibers and nanowires from semiconductors [7], [8] metals [9], [10], [11] and others.

At present, with the introduction of silicon-based nanosystems in technological processes, the most advantageous is the use of templates based on silicon oxide. We can use templates with different pore parameters i.e. diameter, aspect ratio and numerical density as required.

A more economical method is silicon oxide templates (pore diameters ~ 100 nm), which is possible by using porous silicon [12] or direct sputtering of porous a-SiO_2 by plasma chemical vapor deposition [12], [13]. To date, the potential of this type of technique to create templates from porous

a-SiO2 layers on Si has already been extensively investigated [14], [15], [16], [17], [18], [19], [20], [21].

The pores in the SiO_2 layer are formed using track technology, which includes fast heavy ion irradiation (FHI) and chemical etching process [18], [22]. Next, the process of filling the nanopores with different materials is carried out. In our case, we consider the deposition of tin dioxide.

Tin (VI) oxide is a semiconducting oxide with n-type conductivity. Its unique electrical and optical properties make it a promising material. In addition, SnO_2 has a number of excellent properties such as low electrical resistance, high electrical conductivity and high optical transparency in the visible electromagnetic range, and such properties of this material offer opportunities to utilize them in the development of novel applications for nanodevices.

Compared with other semiconductors, SnO_2 is an important functional material which is widely used in transparent conductors [23], transistors [24], optoelectronic devices [25], [26] gas sensors [27], etc.

Today, the templating method [28], hydrothermal method [29], chemical vapor deposition (CVD) [30], [31] and electrochemical deposition [32] are used to synthesize SnO_2 nanostructures with different morphologies.

In our work, we chose the templating synthesis method to fill or produce tin dioxide (SnO_2) nanowires in SiO_2/Si track templates. This synthesis method is considered more economical to obtain such heterostructures ($SnO_2/SiO_2/Si$) with SnO_2 nanopore filling. Our chosen template synthesis is based on chemical and electrochemical deposition of materials into nanoporous substrates. An attractive aspect of template synthesis, is the possibility to tailor the physical, chemical and electronic properties of the nanomaterial by controlled manipulation of morphology, pore density, shape and size. The aim of the research conducted in this work is to form nanowires with orthorhombic crystal structure by controlling the resulting properties. Controlling the morphology of SnO_2 nanomaterials can improve their performance and expand their range of applications to create devices that solve new problems.

2. Methods

In the present work, the SiO_2/Si structure, (n - type) formed by thermal oxidation of silicon crystals in a humid oxygen atmosphere (900℃) was used. According to the data obtained by ellipsometry, the thickness of the oxide layer is 700 nm. To create discontinuous tracks in the SiO_2 matrix, the prepared samples were irradiated on a DC-60 gas pedal, with 132Xe ions with an energy of 200 MeV, the fluence value was in the range of 107 - 108 cm^{-2}.

A 4% aqueous solution of hydrofluoric acid (HF) with m(Pd)=0.025 g was used to form nanoporous templates in the samples irradiated with fast heavy ions (BTI). Etching was performed at room temperature for a certain time under a special fume hood. The size of the nanopores was adjusted depending on the etching time. After the treatment process in HF solution, the samples underwent a washing step in deionized water.

In the present work, chemical precipitation (CP) method was used to fill the nanopores. Chemical deposition is a widely used method for the deposition of semiconductor oxide nanowires (NWs) in SiO_2 nanopores. For deposition, a solution of a coordination compound of a metal and a reducing agent must be used. Unlike the electrochemical method, this method does not require an electrochemically conducting surface. The process starts with the deposition of material on the pore walls, resulting in the formation of a hollow tube inside each pore when the deposition time is short, and when the deposition time is long, solid nanowires are formed. This method does not require any special equipment and is considered low cost, all the components for the deposition of semiconductor oxide nanowires are dissolved in 100 ml of deionized water using magnetic stirrer at a certain time [33].

To obtain tin dioxide (SnO_2) nanowires using the CW method, a sulfate solution with the following composition was used: 0.67 g tin sulfate ($SnSO_4$) + 4 g thiourea (CH_4N_2S) + 2 mL sulfuric acid (H2SO4). CH_4N_2S was pre-dissolved in deionized water and SnSO4 was in turn dissolved in a

minimal volume of concentrated sulfuric acid (hh). The two solutions were then combined, and the pH value of the solution was adjusted in the range of values from 2 to 4 in order to optimize the conditions for the precipitation process. The CW process was carried out at a temperature of 323 K. The process was carried out under thorough mixing conditions using a LOIP LS-110 orbital shaker, to ensure uniform distribution of the reagents and to achieve the desired deposition density.

Detailed study of the obtained nanowires (nanostructures) and interpretation of the measurement results requires the use of modern developments in the field of measuring and diagnostic equipment. Scanning electron microscopy (SEM) and X-ray diffraction analysis (XRD) techniques are the main methods to investigate the structural features and surface morphologies of nanomaterials.

To analyze the pore-filled, as well as to investigate the structural features and surface morphology of SiO_2/Si track templates, after CW, the samples were examined using a Zeiss Crossbeam 540 dual-beam scanning microscope (SEM, Germany) at 2-5 kV equipped with a backscattered electron detector.

Using the X-ray diffraction analysis (XRD) technique, complete information on various properties as well as on the phase composition of the $SnO_2/SiO_2/Si$ structures was obtained. The PCA spectra were identified using a Rigaku SmartLab X-ray diffractometer equipped with a HyPix3000 high-energy 2D HPAD detector. Using TOPAS 4.2 software and the international ICDD database (PDF-2 Release 2020 RDB), standard phase composition determination and determination of crystal cell parameters based on the obtained diffractograms are carried out.

Luminescence spectra at room temperature in the spectral range of 300 to 800 nm with 240 nm excitation were recorded using a CM2203 spectrofluorimeter. The spectrofluorimeter provides highly sensitive measurements in the ultraviolet and visible spectral range. The use of two double monochromators provides a minimum level of interfering radiation, which guarantees high accuracy of measurements.

A VersaStat 3 potentiostat was used to investigate the electrical properties of the arrays of the obtained nanowires. This instrument supports maximum current up to ±2 A, voltage up to ±12 V. The volt-ampere characteristics were taken from an array of 0.7 cm2 filled nanochannels. The setup for measuring the VAC was assembled as follows: the sample was placed between two metal plates, to ensure that the plates cover only the part of the matrix that contains the nanowires. The plates were then connected to a power source by connecting a potentiostat in series. All VACs were performed using a 2nd order polynomial approximation [34].

3. Results and Discussion

Figure 1 shows the SEM pattern of the template surface after chemical deposition.

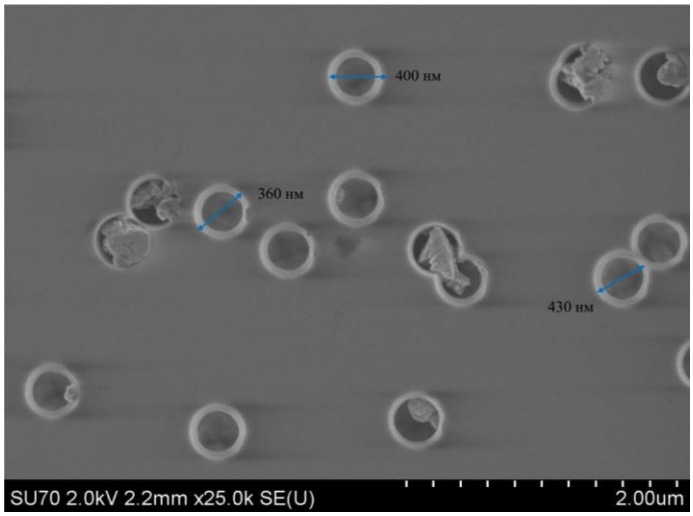

Figure 1 - SEM image of SiO2/Si-n template surface after SnO2 CW (tossing= 20 min, T = 323 K)

As can be seen in Figure 1, the filled nanochannels can be clearly seen when chemically deposited for 20 min. From the analysis of SEM images (Figure 2), we can see that the diameter of nanopores varies between 350 nm and 430 nm. The filling degree of the nanochannels is 80%.

According to the PCA data (Figure 2), chemical precipitation in sulfate solution in SiO_2/Si track templating led to the formation of SnO_2 nanowires with orthorhombic structure and spatial symmetry group Pnnm(58), also appeared Sn phase with tetragonal structure and spatial symmetry group I4/mmm (139).

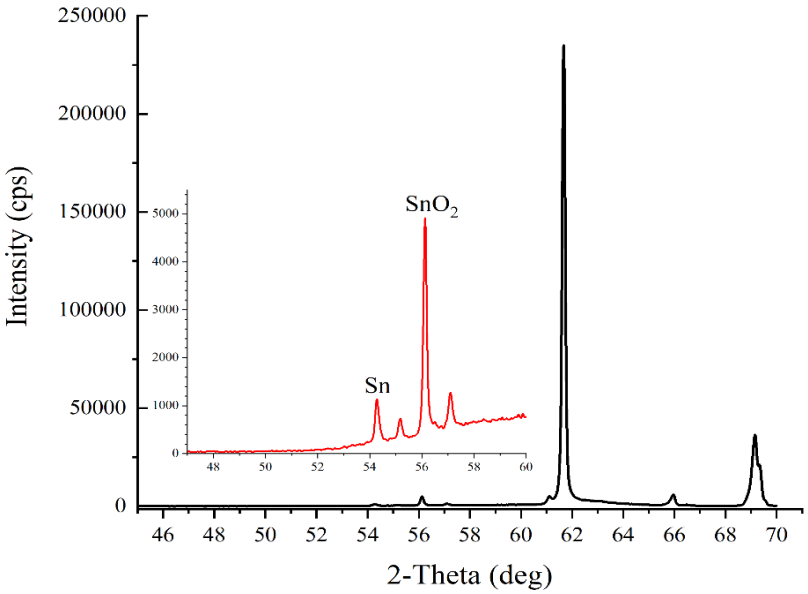

Figure 2 - X-ray diffractogram of SnO_2 samples obtained by CW method for 20 minutes

The results of X-ray diffraction analysis for this sample are shown in Table 1.

Table 1 – Crystallographic parameters of SnO_2 nanowires in SiO_2/Si-n track templated SiO_2/Si-n by PCA results

Phase name	Sn	SnO_2
Type of structure	Tetragonal	Orthorhombic
Prostrate group	139: I4/mmm	58: Pnnm
(hkl)	(002)	(220)
2θ	54.271	56.113
d, Å	1.6889	1.6377
L, nm	648	637
FWHM	0.144	0.15
Lattice parameters, Å	a(A) = 3.674736;	a(A) = 4.655800;
Volume, Å3	b(A) = 3.674736;	b(A) = 4.599800;
Crystallite size, $Å^3$	c(A) = 3.377628	c(A) = 3.151400
Density, g/cm^3	45.610417	67.489592

According to the results of X-ray diffraction analysis, we can conclude that the concentration ratio of Sn phase to SnO_2 phase is 22% by 78%, respectively.

The cell parameters obtained in experimental [35], [36] and theoretical works [37] are in good agreement with the data obtained for our orthorhombic tin dioxide nanowires.

Optical investigation techniques such as photoluminescence (PL) were used to determine the defects and impurities in the obtained nanowires. The photoluminescence (PL) of SnO_2-NP/SiO_2/Si nanostructure was investigated in the spectral range of 2 - 3.2 eV when excited by light with wavelength λ = 5.17 eV. Figure 3 shows the Gaussian decomposition of the photoluminescence spectrum of SnO_2-NP/SiO_2/Si structures obtained by chemical deposition. SiO_2 luminescence is taken into account in the photoluminescence spectrum.

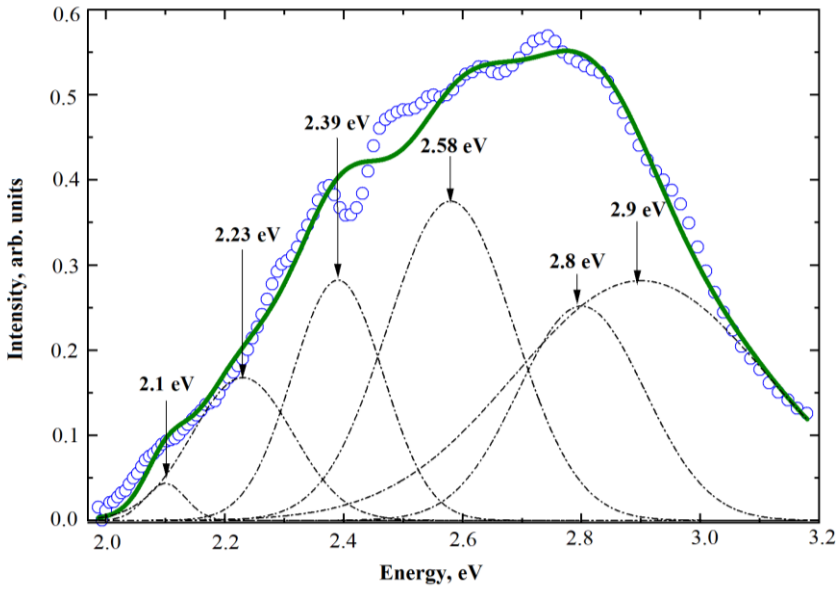

Figure 3 – Gaussian decomposition of the photoluminescence spectrum of SnO_2-NP/SiO_2/Si structures

The PL spectra of nanowires obtained by chemical deposition show differences compared to the PL spectra of nanowires synthesized by electrochemical method, characterized by higher intensity maxima. Impurities and defects present in the material due to different synthesis method, solutions used and temperature may play a key role in the variation of the intensity of the PL spectra. The observed intense peaks at 2.9 eV, 2.8 eV, 2.58 eV, 2.39 eV, 2.23 eV, 2.1 eV on the luminescence spectrum agree well with the results of similar measurements by researchers [38]. It is widely known from the authors [39], the emission of visible light is related to the energy levels of defects in the forbidden band of SnO2 associated with O-vacancies and Sn interstitials. The luminescence centers responsible for the violet emission maximum at 2.9 eV can be attributed to interstitial tin or tin with damaged bonds [40], [41], [42], [43], [44]. The blue light emission with a maximum at 2.8 eV can be due to the transition from the triplet state to the ground state for V_O^0 [45]. Most of the oxygen vacancies are in the paramagnetic state of V_O^+ with a peak at 2.58 eV [46], [42] and the peak at 2.39 eV [47] corresponds to the surface donor V_O^0. The 2.23 eV peak is probably the result of oxygen vacancies that are formed during the deposition process as indicated by [48], [49]. The maximum at 2.1 eV is related to defect levels in the forbidden band associated with O vacancies or interstitial Sn, which was observed in the case of SnO2 nanoribbons synthesized by laser ablation [50] and SnO_2 nanorods that were obtained by growth from solution phase [51]. It is widely known that oxygen vacancies are the most frequent type of defects and often act as emitting defects in the occurrence of luminescence. Indeed, the analysis of the FL spectrum shows that it is oxygen vacancies rather than tin-related defects that are the main defects.

The study of the voltammetric characteristic of the SnO_2-NP/SiO_2/Si structure allows us to determine the type of conductivity of the synthesized structure. The voltammetric characteristic (VAC) was measured from an array of filled nanochannels with an area of 0.7 cm². Figure 4 presents the VAC of the samples before and after deposition, demonstrating the influence of the synthesis process on the electrical properties of the structure.

The obtained VAC exhibits a nonlinear, asymmetric shape, indicating a deviation from ideal ohmic behavior. This suggests the presence of a Schottky barrier or other charge transport mechanisms influenced by the material's defect structure and metallic inclusions.

The curve shows an increase in conductivity after deposition, which can be attributed to the incorporation of metallic tin, leading to enhanced charge carrier mobility. In the negative voltage region, a pronounced increase in current is observed, further supporting the presence of metallic conductivity components.

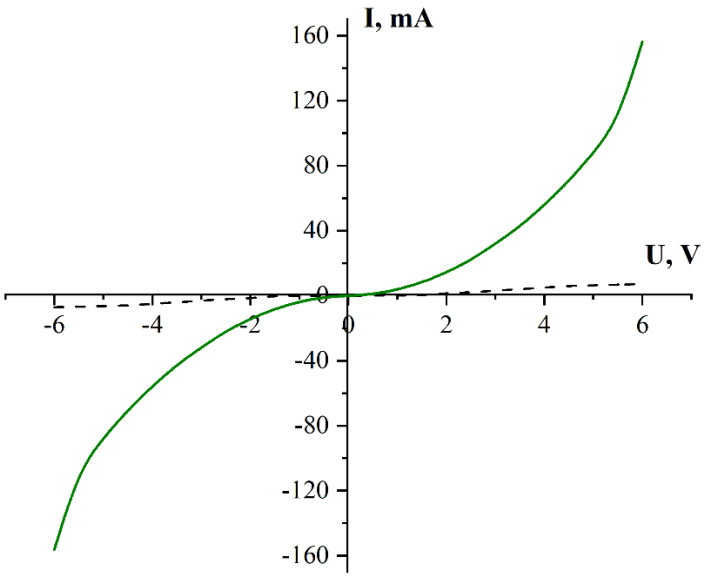

Figure 4 – Volt-ampere characteristic of SnO_2-NP/SiO_2/Si: dotted curve - original sample; solid curve - with deposited SnO_2 (tossing= 20 min, T = 323 K)

Overall, the results highlight the impact of structural modifications on the electronic properties of the SnO_2-NP/SiO_2/Si system, emphasizing the role of metallic tin in altering the charge transport mechanism.

4. Conclusions

In this study, tin dioxide (SnO_2) nanowires were synthesized by chemical deposition into SiO_2/Si track templates. X-ray structural analysis confirmed that the obtained nanowires exhibit an orthorhombic crystal structure with lattice parameters: a = 4.655800 Å, b = 4.599800 Å, c = 3.151400 Å. Additionally, the presence of metallic tin was detected, which significantly influences their physicochemical properties.

Photoluminescence spectrum analysis revealed a broad emission band in the energy range from 2 eV to 3.2 eV, indicating the complex nature of radiative processes. Investigation of the defect structure showed that the dominant point defects are oxygen vacancies, which play a key role in shaping the optical properties of the material. Moreover, spectral maxima associated with interdomain tin atoms and tin with broken chemical bonds were identified. These defects can act as effective recombination centers and influence the mechanisms of charge carrier generation and relaxation.

Analysis of the current-voltage characteristics (I-V curves) of SnO_2 nanowires with an orthorhombic crystal structure demonstrated that, due to the presence of metallic tin, their conductivity approaches a metallic type. This indicates a significant modification of the electronic structure compared to pure tin dioxide, which typically exhibits semiconductor properties. The presence of metallic inclusions may contribute to the formation of tunneling junctions and localized conductive channels, making such nanostructures promising for applications in nanoelectronics, sensing, and hybrid electronic devices.

Thus, the obtained results demonstrate the possibility of precisely controlling the structural, optical, and electrical properties of SnO_2 nanowires through the incorporation of metallic tin, opening new prospects for their practical applications.

References

[1] D. V. Talapin, J. S. Lee, M. V. Kovalenko, and E. V. Shevchenko, “Prospects of colloidal nanocrystals for electronic and optoelectronic applications,” *Chem. Rev.*, vol. 110, no. 1, pp. 389–458, Jan. 2010, doi: 10.1021/CR900137K/ASSET/IMAGES/CR-2009-00137K_M028.GIF.

[2] “(PDF) Nanotechnology, Big things from a Tiny World: a Review.” Accessed: Mar. 13, 2025. [Online]. Available:

https://www.researchgate.net/publication/46189710_Nanotechnology_Big_things_from_a_Tiny_World_a_Review
[3] W. Lu and C. M. Lieber, "Nanoelectronics from the bottom up," *Nat. Mater. 2007 611*, vol. 6, no. 11, pp. 841–850, 2007, doi: 10.1038/nmat2028.
[4] M. R. Jones, K. D. Osberg, R. J. MacFarlane, M. R. Langille, and C. A. Mirkin, "Templated techniques for the synthesis and assembly of plasmonic nanostructures," *Chem. Rev.*, vol. 111, no. 6, pp. 3736–3827, Jun. 2011, doi: 10.1021/CR1004452/ASSET/CR1004452.FP.PNG_V03.
[5] D. Routkevitch, T. Bigioni, M. Moskovits, and J. M. Xu, "Electrochemical Fabrication of CdS Nanowire Arrays in Porous Anodic Aluminum Oxide Templates," *J. Phys. Chem.*, vol. 100, no. 33, pp. 14037–14047, Aug. 1996, doi: 10.1021/JP952910M.
[6] F. Zhang and D. Zhao, "Fabrication of ordered magnetite-doped rare earth fluoride nanotube arrays by nanocrystal self-assembly," *Nano Res.*, vol. 2, no. 4, pp. 292–305, Apr. 2009, doi: 10.1007/S12274-009-9027-6/METRICS.
[7] "Preparation of CdS Single-Crystal Nanowires by Electrochemically Induced Deposition - Xu - 2000 - Advanced Materials - Wiley Online Library." Accessed: Mar. 13, 2025. [Online]. Available: https://advanced.onlinelibrary.wiley.com/doi/10.1002/%28SICI%291521-4095%28200004%2912%3A7%3C520%3A%3AAID-ADMA520%3E3.0.CO%3B2-%23
[8] C. R. Martin, "Nanomaterials: A Membrane-Based Synthetic Approach," *Science (80-.).*, vol. 266, no. 5193, pp. 1961–1966, Dec. 1994, doi: 10.1126/SCIENCE.266.5193.1961.
[9] I. U. Schuchert, M. E. T. Molares, D. Dobrev, J. Vetter, R. Neumann, and M. Martin, "Electrochemical Copper Deposition in Etched Ion Track Membranes : Experimental Results and a Qualitative Kinetic Model," *J. Electrochem. Soc.*, vol. 150, no. 4, p. C189, Feb. 2003, doi: 10.1149/1.1554722.
[10] S. E. Demyanov *et al.*, "On the morphology of Si/SiO2/Ni nanostructures with swift heavy ion tracks in silicon oxide," *J. Surf. Investig.*, vol. 8, no. 4, pp. 805–813, Aug. 2014, doi: 10.1134/S1027451014040326/METRICS.
[11] V. Sivakov *et al.*, "Silver nanostructures formation in porous Si/SiO2 matrix," *J. Cryst. Growth*, vol. 400, pp. 21–26, Aug. 2014, doi: 10.1016/J.JCRYSGRO.2014.04.024.
[12] A. Barranco, J. Cotrino, F. Yubero, J. P. Espinós, and A. R. González-Elipe, "Room temperature synthesis of porous SiO2 thin films by plasma enhanced chemical vapor deposition," *J. Vac. Sci. Technol. A*, vol. 22, no. 4, pp. 1275–1284, Jul. 2004, doi: 10.1116/1.1761072.
[13] G. Amato, S. Borini, A. M. Rossi, L. Boarino, and M. Rocchia, "Si/SiO2 nanocomposite by CVD infiltration of porous SiO2," *Phys. status solidi*, vol. 202, no. 8, pp. 1529–1532, Jun. 2005, doi: 10.1002/PSSA.200461172.
[14] D. Fink, A. Chandra, P. Alegaonkar, A. Berdinsky, A. Petrov, and D. Sinha, "Nanoclusters and nanotubes for swift ion track technology," *Radiat. Eff. Defects Solids*, vol. 162, no. 3–4, pp. 151–156, Mar. 2007, doi: 10.1080/10420150601132487.
[15] Y. A. Ivanova *et al.*, "Electrochemical deposition of Ni and Cu onto monocrystalline n-Si(100) wafers and into nanopores in Si/SiO2 template," *J. Mater. Sci.*, vol. 42, no. 22, pp. 9163–9169, Nov. 2007, doi: 10.1007/S10853-007-1926-X/METRICS.
[16] K. Hoppe *et al.*, "An ion track based approach to nano- and micro-electronics," *Nucl. Instruments Methods Phys. Res. Sect. B Beam Interact. with Mater. Atoms*, vol. 266, no. 8, pp. 1642–1646, Apr. 2008, doi: 10.1016/J.NIMB.2007.12.069.
[17] A. Razpet, A. Johansson, G. Possnert, M. Skupiński, K. Hjort, and A. Hallén, "Fabrication of high-density ordered nanoarrays in silicon dioxide by MeV ion track lithography," *J. Appl. Phys.*, vol. 97, no. 4, Feb. 2005, doi: 10.1063/1.1850617/914557.
[18] A. Dallanora *et al.*, "Nanoporous SiO2/Si thin layers produced by ion track etching: Dependence on the ion energy and criterion for etchability," *J. Appl. Phys.*, vol. 104, no. 2, Jul. 2008, doi: 10.1063/1.2957052/936055.
[19] "Characteristic features of electric charge transfer processes in Si/SiO2/Ni nanostructures in strong magnetic fields | Request PDF." Accessed: Mar. 13, 2025. [Online]. Available: https://www.researchgate.net/publication/290999855_Characteristic_features_of_electric_charge_transfer_processes_in_SiSiO2Ni_nanostructures_in_strong_magnetic_fields
[20] L. A. Vlasukova *et al.*, "Threshold and criterion for ion track etching in SiO2 layers grown on Si," *Vacuum*, vol. 105, pp. 107–110, Jul. 2014, doi: 10.1016/J.VACUUM.2014.01.005.
[21] A. Benyagoub and M. Toulemonde, "Ion tracks in amorphous silica," *J. Mater. Res.*, vol. 30, no. 9, pp. 1529–1543, Jan. 2015, doi: 10.1557/JMR.2015.75/METRICS.
[22] E. Kaniukov, V. Bundyukova, M. Kutuzau, and D. Yakimchuk, "Peculiarities of formation and characterization of SiO2/Si ion-track template," *NATO Sci. Peace Secur. Ser. B Phys. Biophys.*, pp. 41–57, 2019, doi: 10.1007/978-94-024-1687-9_3.
[23] A. Vaseashta and D. Dimova-Malinovska, "Nanostructured and nanoscale devices, sensors and detectors," *Sci. Technol. Adv. Mater.*, vol. 6, no. 3-4 SPEC. ISS., pp. 312–318, Apr. 2005, doi: 10.1016/J.STAM.2005.02.018.
[24] J. C. Chou and Y. F. Wang, "Preparation and study on the drift and hysteresis properties of the tin oxide gate ISFET by the sol–gel method," *Sensors Actuators B Chem.*, vol. 86, no. 1, pp. 58–62, Aug. 2002, doi: 10.1016/S0925-4005(02)00147-8.
[25] J. S. Lee, S. K. Sim, B. Min, K. Cho, S. W. Kim, and S. Kim, "Structural and optoelectronic properties of SnO2 nanowires synthesized from ball-milled SnO2 powders," *J. Cryst. Growth*, vol. 267, no. 1–2, pp. 145–149, Jun. 2004, doi: 10.1016/J.JCRYSGRO.2004.03.030.

[26] Z. Ying, Q. Wan, Z. T. Song, and S. L. Feng, "Controlled synthesis of branched SnO2 nanowhiskers," *Mater. Lett.*, vol. 59, no. 13, pp. 1670–1672, Jun. 2005, doi: 10.1016/J.MATLET.2005.01.044.
[27] Y. Fan, J. Liu, H. Lu, P. Huang, and D. Xu, "Hierarchical structure SnO2 supported Pt nanoparticles as enhanced electrocatalyst for methanol oxidation," *Electrochim. Acta*, vol. 76, pp. 475–479, Aug. 2012, doi: 10.1016/J.ELECTACTA.2012.05.067.
[28] H. Zhang *et al.*, "Preparation of SnO2 Nanowires by Solvent-Free Method Using Mesoporous Silica Template and Their Gas Sensitive Properties," *J. Nanosci. Nanotechnol.*, vol. 11, no. 12, pp. 11114–11118, 2011, doi: 10.1166/JNN.2011.3978.
[29] H. Zhang, Q. He, X. Zhu, D. Pan, X. Deng, and Z. Jiao, "Surfactant-free solution phase synthesis of monodispersed SnO2 hierarchical nanostructures and gas sensing properties," *CrystEngComm*, vol. 14, no. 9, pp. 3169–3176, Apr. 2012, doi: 10.1039/C2CE06558D.
[30] L. Yu, L. Zhang, H. Song, X. Jiang, and Y. Lv, "Hierarchical SnO2 architectures: controllable growth on graphene by atmospheric pressure chemical vapour deposition and application in cataluminescence gas sensor," *CrystEngComm*, vol. 16, no. 16, pp. 3331–3340, Mar. 2014, doi: 10.1039/C3CE42538J.
[31] H. Huang, O. K. Tan, Y. C. Lee, T. D. Tran, M. S. Tse, and X. Yao, "Semiconductor gas sensor based on tin oxide nanorods prepared by plasma-enhanced chemical vapor deposition with postplasma treatment," *Appl. Phys. Lett.*, vol. 87, no. 16, pp. 1–3, Oct. 2005, doi: 10.1063/1.2106006/910140.
[32] J. Pan *et al.*, "SnO2-TiO2 Core-shell nanowire structures: Investigations on solid state reactivity and photocatalytic behavior," *J. Phys. Chem. C*, vol. 115, no. 35, pp. 17265–17269, Sep. 2011, doi: 10.1021/JP201901B/ASSET/IMAGES/MEDIUM/JP-2011-01901B_0009.GIF.
[33] A. K. Dauletbekova, A. Y. Alzhanova, A. T. Akilbekov, A. A. Mashentseva, M. V. Zdorovets, and K. N. Balabekov, "Synthesis of Si/SiO2/ZnO nanoporous materials using chemical and electrochemical deposition techniques," *AIP Conf. Proc.*, vol. 1767, no. 1, Sep. 2016, doi: 10.1063/1.4962589/755185.
[34] A. Dauletbekova *et al.*, "Ion-Track Template Synthesis and Characterization of ZnSeO3 Nanocrystals," *Cryst. 2022, Vol. 12, Page 817*, vol. 12, no. 6, p. 817, Jun. 2022, doi: 10.3390/CRYST12060817.
[35] J. Haines and J. Léger, "X-ray diffraction study of the phase transitions and structural evolution of tin dioxide at high pressure:ffRelationships between structure types and implications for other rutile-type dioxides," *Phys. Rev. B*, vol. 55, no. 17, p. 11144, May 1997, doi: 10.1103/PhysRevB.55.11144.
[36] S. R. Shieh, A. Kubo, T. S. Duffy, V. B. Prakapenka, and G. Shen, "High-pressure phases in SnO2 to 117 GPa," *Phys. Rev. B - Condens. Matter Mater. Phys.*, vol. 73, no. 1, p. 014105, Jan. 2006, doi: 10.1103/PHYSREVB.73.014105/FIGURES/6/THUMBNAIL.
[37] L. Gracia, A. Beltrán, and J. Andrés, "Characterization of the High-Pressure Structures and Phase Transformations in SnO2. A Density Functional Theory Study," *J. Phys. Chem. B*, vol. 111, no. 23, pp. 6479–6485, Jun. 2007, doi: 10.1021/JP067443V.
[38] B. Wang and P. Xu, "Growth mechanism and photoluminescence of the SnO2 nanotwists on thin film and the SnO2 short nanowires on nanorods," *Chinese Phys. B*, vol. 18, no. 1, p. 324, Jan. 2009, doi: 10.1088/1674-1056/18/1/053.
[39] E. J. H. Lee, C. Ribeiro, T. R. Giraldi, E. Longo, E. R. Leite, and J. A. Varela, "Photoluminescence in quantum-confined SnO2 nanocrystals: Evidence of free exciton decay," *Appl. Phys. Lett.*, vol. 84, no. 10, pp. 1745–1747, Mar. 2004, doi: 10.1063/1.1655693.
[40] S. Munnix and M. Schmeits, "Electronic structure of tin dioxide surfaces," *Phys. Rev. B*, vol. 27, no. 12, p. 7624, Jun. 1983, doi: 10.1103/PhysRevB.27.7624.
[41] N. Chiodini, A. Paleari, D. Dimartino, and G. Spinolo, "SnO2 nanocrystals in SiO2: A wide-band-gap quantum-dot system," *Appl. Phys. Lett.*, vol. 81, no. 9, pp. 1702–1704, Aug. 2002, doi: 10.1063/1.1503154.
[42] K. Vanheusden, W. L. Warren, C. H. Seager, D. R. Tallant, J. A. Voigt, and B. E. Gnade, "Mechanisms behind green photoluminescence in ZnO phosphor powders," *J. Appl. Phys.*, vol. 79, no. 10, pp. 7983–7990, May 1996, doi: 10.1063/1.362349.
[43] Y. Liu, Q. Yang, and C. Xu, "Single-narrow-band red upconversion fluorescence of ZnO nanocrystals codoped with Er and Yb and its achieving mechanism," *J. Appl. Phys.*, vol. 104, no. 6, Sep. 2008, doi: 10.1063/1.2980326/343684.
[44] K. G. Godinho, A. Walsh, and G. W. Watson, "Energetic and Electronic Structure Analysis of Intrinsic Defects in SnO2," *J. Phys. Chem. C*, vol. 113, no. 1, pp. 439–448, Jan. 2008, doi: 10.1021/JP807753T.
[45] Y. C. Her, J. Y. Wu, Y. R. Lin, and S. Y. Tsai, "Low-temperature growth and blue luminescence of SnO2 nanoblades," *Appl. Phys. Lett.*, vol. 89, no. 4, Jul. 2006, doi: 10.1063/1.2235925/986618.
[46] S. Rani, S. C. Roy, N. Karar, and M. C. Bhatnagar, "Structure, microstructure and photoluminescence properties of Fe doped SnO2 thin films," *Solid State Commun.*, vol. 141, no. 4, pp. 214–218, Jan. 2007, doi: 10.1016/J.SSC.2006.10.036.
[47] M. Bhatnagar, V. Kaushik, A. Kaushal, M. Singh, and B. R. Mehta, "Structural and photoluminescence properties of tin oxide and tin oxide: C core-shell and alloy nanoparticles synthesised using gas phase technique," *AIP Adv.*, vol. 6, no. 9, p. 95321, Sep. 2016, doi: 10.1063/1.4964313/884807.
[48] J. Duan *et al.*, "Multiform structures of SnO2 nanobelts," *Nanotechnology*, vol. 18, no. 5, p. 055607, Jan. 2007, doi: 10.1088/0957-4484/18/5/055607.
[49] L. Zhang, S. Ge, Y. Zuo, B. Zhang, and L. Xi, "Influence of oxygen flow rate on the morphology and magnetism of SnO 2 nanostructures," *J. Phys. Chem. C*, vol. 114, no. 17, pp. 7541–7547, May 2010, doi:

10.1021/JP9065604/ASSET/IMAGES/MEDIUM/JP-2009-065604_0007.GIF.
[50] J. Hu, Y. Bando, Q. Liu, and D. Golberg, "Laser-Ablation Growth and Optical Properties of Wide and Long Single-Crystal SnO2 Ribbons," *Adv. Funct. Mater.*, vol. 13, no. 6, pp. 493–496, Jun. 2003, doi: 10.1002/ADFM.200304327.
[51] B. Cheng, J. M. Russell, W. Shi, L. Zhang, and E. T. Samulski, "Large-Scale, Solution-Phase Growth of Single-Crystalline SnO2 Nanorods," *J. Am. Chem. Soc.*, vol. 126, no. 19, pp. 5972–5973, May 2004, doi: 10.1021/JA0493244/SUPPL_FILE/JA0493244SI20040402_033424.PDF.

Information about authors:

Diana Junisbekova – Doctor PhD, Senior Lecturer, Faculty of Physics and Technical Sciences, L.N. Gumilyov Eurasian National University, Astana, Kazakhstan, diana911115@gmail.com
Zein Baimukhanov – Candidate of Physical and Mathematical Sciences, Acting Associate Professor, Faculty of Physics and Technical Sciences, L.N. Gumilyov Eurasian National University, Astana, Kazakhstan, baimukhanov_zk@enu.kz
Alma Dauletbekova – Doctor of Physical and Mathematical Sciences, Professor, Faculty of Physics and Technical Sciences, L.N. Gumilyov Eurasian National University, Astana, Kazakhstan, dauletbekova_ak@enu.kz

Author Contributions:

Diana Junisbekova – data collection, testing, modeling, analysis, visualization.
Zein Baimukhanov – interpretation, drafting, editing, funding acquisition.
Alma Dauletbekova – concept, methodology, resources.

Received: *03.02.2025*
Revised: 26.02.2025
Accepted: 17.03.2025
Published: 18.03.2025

Conflict of Interest: The authors declare no conflict of interest.

Use of Artificial Intelligence (AI): The authors declare that AI was not used.